Type of contribution:
Editorial
▶ Research Paper
Case Study
Review Paper
Scientific Data
Report of Tech. Application

e-issn. 2798-5245

Mechanical Engineering for Society and Industry
Vol. 5, No. 2 (2025) pp 353-366
https://doi.org/10.31603/mesi.13588

Smart vibration sensing and predictive analytics for intelligent textile manufacturing: An IoT-edge and machine learning method

Deni Kurnia[1,2], Agus Sutanto[1]*, Hanif Fakhrurroja[3], Lovely Son[1]

[1] Department of Mechanical Engineering, Universitas Andalas, Padang 25163, **Indonesia**
[2] Department of Mechatronics Engineering, Politeknik Enjinering Indorama, Purwakarta 41152, **Indonesia**
[3] Research Center for Smart Mechatronics, BRIN, Bandung 40135, **Indonesia**
✉ agussutanto@eng.unand.ac.id

Highlights:

- IoT-Edge system detects vibration faults in DTY machines using ADXL345 and ML models.
- Tuned Random Forest achieved 97% accuracy, outperforming SVM baseline (71%).
- Low-latency (20.37 ms) MQTT ensures real-time, scalable predictive maintenance.

Abstract

This study aimed to propose an IoT-Edge method for detecting vibration abnormalities in Textile Manufacturing, specifically on Draw Texturing Yarn (DTY) machines using an ADXL345 sensor and a Machine Learning Algorithm. The proposed system incorporated wireless sensor nodes, the MQTT protocol, Fast Fourier Transform (FFT) analysis, and a tuned Random Forest (RF) classifier to enable real-time monitoring as well as predictive maintenance. During the analysis, vibration data were collected from 13 spindles, with features extracted in both time as well as frequency domains to distinguish between normal and abnormal machine conditions. The RF model, optimized through hyperparameter tuning, achieved an accuracy of 97%, significantly outperforming the Support Vector Machine (SVM) baseline, which reached 71%. Major results showed the effectiveness of energy and centroid features in fault detection, with the Z-axis vibration proving to be a good indicator of yarn defects. The system presented low latency (average 20.37 ms) in data transmission using the MQTT protocol, ensuring practical deployability. This study offered a scalable and cost-effective solution for industrial vibration monitoring, bridging gaps in real-time processing and seamless IoT incorporation to support predictive maintenance in textile manufacturing.

Keywords: IoT; DTY machine; ADXL345; MQTT; Random forest; Hyperparameter tuning

Article info
Submitted: 2025-05-16
Revised: 2025-09-07
Accepted: 2025-10-15

Publisher
Universitas Muhammadiyah Magelang

1. Introduction

Machine vibration monitoring is a crucial aspect of predictive maintenance in Industry 4.0, especially in industrial sectors such as textile manufacturing, where high-speed machinery, including Draw Texturing Yarn (DTY) equipment is widely used [1], [2], [3]. Abnormal vibration in

DTY machines adversely affect yarn quality by introducing production defects. As a result, existing mitigation strategies depend on conventional methods, which are hindered by high costs, structural inflexibility, and reliance on manual inspection. These limitations lead to delayed fault detection, unpredictable maintenance expenditures, and costly operational disruptions [4].

In recent years, experts have increasingly applied machine learning methods to monitor industrial equipment and predict mechanical failures. Among various methods, vibration signal analysis has become a prominent non-invasive model due to its ability to detect mechanical anomalies efficiently and a straightforward data acquisition process. Recent technological developments have introduced cost-effective alternatives using MEMS accelerometers and microcontrollers [5], [6], alongside machine learning models such as Support Vector Machines (SVM) [7], [8]. Following the discussion, Random Forest (RF) has appeared as a preferred classification algorithm owing to its robustness against overfitting, scalability, and effectiveness in managing high-dimensional datasets [9], [10], [11]. Its intrinsic feature importance assessment capability improves the utility in identifying critical attributes in complex vibration data. Deep learning methods [12], [13], [14], such as Convolutional Neural Networks (CNNs), have also been investigated [15], particularly for handling raw time-series vibration data. Although these models show strong learning capabilities, the methods often require large datasets and substantial computational resources, which can be less practical for industrial applications.

Current systems continue to face challenges in real-time data processing, seamless incorporation of sensor networks and edge computing despite recent advancement. In addition, optimizing machine learning algorithm remains particularly difficult for vibration monitoring in DTY machine vibration. This study addresses the gap by proposing an incorporated IoT framework that combines the ADXL345 accelerometer [16], ESP32 microcontroller [17], and MQTT protocol [18], along with an optimized RF classifier [19]. The proposed system incorporates wireless sensor nodes, Fast Fourier Transform (FFT) analysis via Python, and an advanced hyperparameter tuning algorithm to detect abnormal vibration in DTY machines.

This study distinctively contributes to the field by incorporating a cost-effective IoT-edge architecture (ADXL345, ESP32, MQTT) with a rigorously optimized machine learning pipeline for real-time vibration analysis on live DTY machines. The method is validated using real-world industrial data from 13 operational spindles different from many studies that rely on standardized bearing datasets [7], [8], capturing authentic fault patterns specific to textile manufacturing. Furthermore, the analysis delivers a comprehensive performance evaluation of both the classification model and entire data transmission pipeline, including latency analysis, an aspect often overlooked in similar studies. This holistic, industry-focused method improves both the practical applicability and novelty of the proposed system.

2. Methods

2.1. Block Diagram

During this study, the system architecture was composed of spindle vibration from the DTY machine as a novel data source. A spindle-mounted sensor sent data wirelessly using the MQTT communication protocol incorporated with an ESP32 controller. The server/computer processed the collected data through FFT and the RF machine learning algorithm, as shown in **Figure 1**.

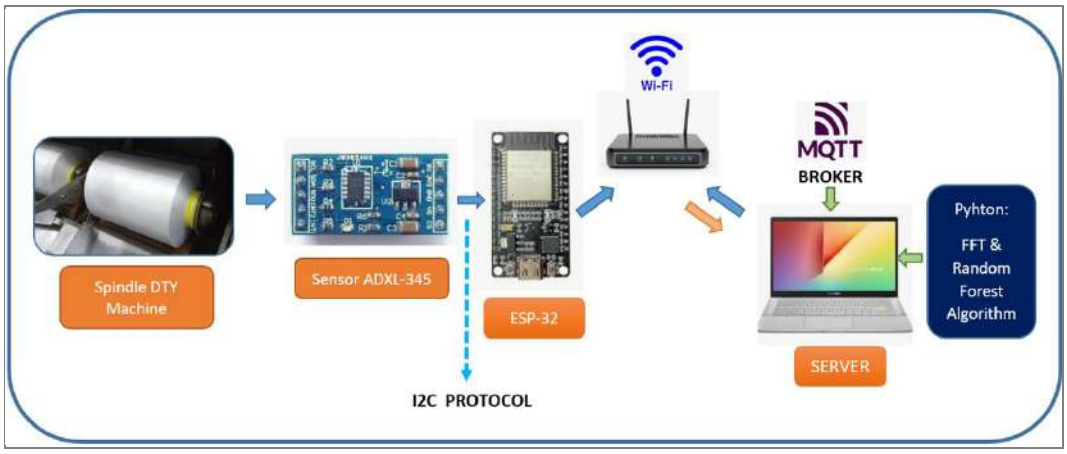

Figure 1. System architecture

2.2. Data Acquisition and FFT Process

Figure 2 showed that vibration data were collected using an ADXL345 accelerometer connected to an ESP32 microcontroller with the I2C protocol [20]. The sensor captured acceleration along the X, Y, and Z axes, which were then transmitted via wireless communication using a local HiveMQ broker hosted on a PC. A Python-based subscriber received and processed the incoming data for analysis and classification, including latency testing. Before data acquisition, the sensor was calibrated to ensure accurate readings.

As a data source, a total of 13 spindles (yarn winders) worked continuously to roll the yarn for approximately 8 hours from start to finish. The data collection process was categorized into two groups based on the source, namely, machine spindles identified with abnormal and those with normal vibration. The criteria for determining normal and abnormal characteristics were derived from field observation of yarn production on spindles, as established in previous studies [21].

Each raw acceleration data set was transformed into the frequency domain using FFT [22]. Using a sample rate of 200 and a sample size of 512, the frequency resolution was 0.39 Hz. The data collection process lasted 2.56 seconds (512/200) when retrieving data from the MQTT broker. The resulting FFT output produced an amplitude spectrum over a range of frequencies, capturing vibration characteristics of the DTY machine.

Figure 2. The process of installing (a) and calibrating (b) the sensor on the DTY machine spindle

2.3. MQTT Latency Measurement

Latency was measured as the time difference between the moment the ESP32 sent a timestamp and the moment it was received by the Python subscriber to evaluate communication performance, which included the following steps.

a. The ESP32 sent a JSON payload containing its local timestamp (in milliseconds) to the topic sensor/esp1_latency.
b. Upon receiving the message, the subscriber recorded the current time and computed the latency as Latency = t received – t sent.
c. This process was repeated for 100 messages with a 5 ms interval (~200 Hz sampling rate).

2.4. Feature Extraction and Automatic Labeling

The acquired vibration signals from the ADXL345 sensor were processed through a systematic pipeline to extract statistically relevant and spectrally discriminative features. The preprocessing stage incorporated signal denoising and amplitude normalization across time-windowed segments to improve data quality. Following the process, comprehensive time-domain feature extraction was conducted for the triaxial components (X, Y, Z), capturing both distributional characteristics and dynamic response patterns. Subsequent frequency-domain transformation via FFT enabled spectral decomposition, facilitating the derivation of distinctive features including predominant

frequency components, spectral entropy measures, and total energy distribution. After the feature extraction was completed, Violin [23] and PCA Plot Analysis were conducted [24] to observe the characteristics of vibration features based on the extracted data.

Each feature vector was annotated with a class label ("0 for Normal" or "1 for Abnormal") to facilitate supervised learning, reflecting the operational status of the DTY spindle machine during data acquisition. Labeling criteria were established through expert evaluation and vibration threshold analysis, ensuring good position with machine stability benchmarks. During the process, the resultant labeled dataset served as the basis for training and validating the classification models.

The initial dataset used in this study comprised 142,592 abnormal and 68,608 normal samples. After balancing, both classes were later standardized to 68,608 samples each. The test set (n=108) was derived through stratified random sampling from the balanced dataset to ensure representative proportions of both classes for final model evaluation. This method prevented bias and provided a reliable estimate of model performance on unseen data. A total of 6 most discriminative features were selected for model training and evaluation, consisting of both time-domain as well as frequency-domain characteristics, as shown in **Table 1**.

Table 1. Features extraction of vibration signal for model training and evaluation

Feature Name	Description	Domain	Units
X_energy	Energy of vibration signal on X-axis	Frequency	$(m/s^2)^2$
Y_energy	Energy of vibration signal on Y-axis	Frequency	$(m/s^2)^2$
Z_energy	Energy of vibration signal on Z-axis	Frequency	$(m/s^2)^2$
X_centroid	Spectral centroid of X-axis vibration	Frequency	Hz
Y_centroid	Spectral centroid of Y-axis vibration	Frequency	Hz
Z_centroid	Spectral centroid of Z-axis vibration	Frequency	Hz

2.5. A Supervised Learning Method

The current stage performed classification of vibration states of the DTY spindle machine based on the extracted feature vectors. The analytical workflow started with dataset partitioning, applying an 80:20 stratified split ratio to create distinct training and evaluation subsets, thereby ensuring robust model generalization. The training subset facilitated model development and optimization, while the testing subset served for final performance assessment.

RF algorithm was adopted as the primary classifier during the process, leveraging its shown robustness, inherent interpretability, and effectiveness with high-dimensional feature spaces [25], [26], [27]. For comparative analysis, an SVM model was implemented as a baseline reference under identical data conditions [28], [29], [30]. Model efficacy was quantified through comprehensive metrics, including classification accuracy, precision, recall, and F1-score, all derived from respective confusion matrices.

2.6. Hyperparameter Tuning

RF classifier passed through systematic hyperparameter optimization via Grid Search CV to improve predictive performance [31]. The search space comprised critical parameters including n_estimators, max_depth, criterion, and min_samples_split. The optimal configuration, determined by Cross-Validation [32], was subsequently retrained on the complete training dataset. Computational efficiency was rigorously evaluated through comparative timing analysis of the training phase, providing perceptions into both predictive accuracy and operational practicality.

2.7. Evaluation and Visualization

Final model validation included visual interpretation through confusion matrix analysis and comparative metric visualization, conclusively showing the tuned superior performance of the RF classifier relative to the SVM baseline for the target vibration classification task. All stages in this method section were shown in **Figure 3**.

3. Results and Discussion

3.1. Results

The results of data acquisition were 142,592 vibration data from abnormal spindles and 68,608 from normal spindles. **Figure 4** showed the sample data comparison from each spindle on

the Z-axis. The Z-axis was selected because, according to a previous study [21], vibration changes on this axis were dominant cause of yarn defects in DTY machines.

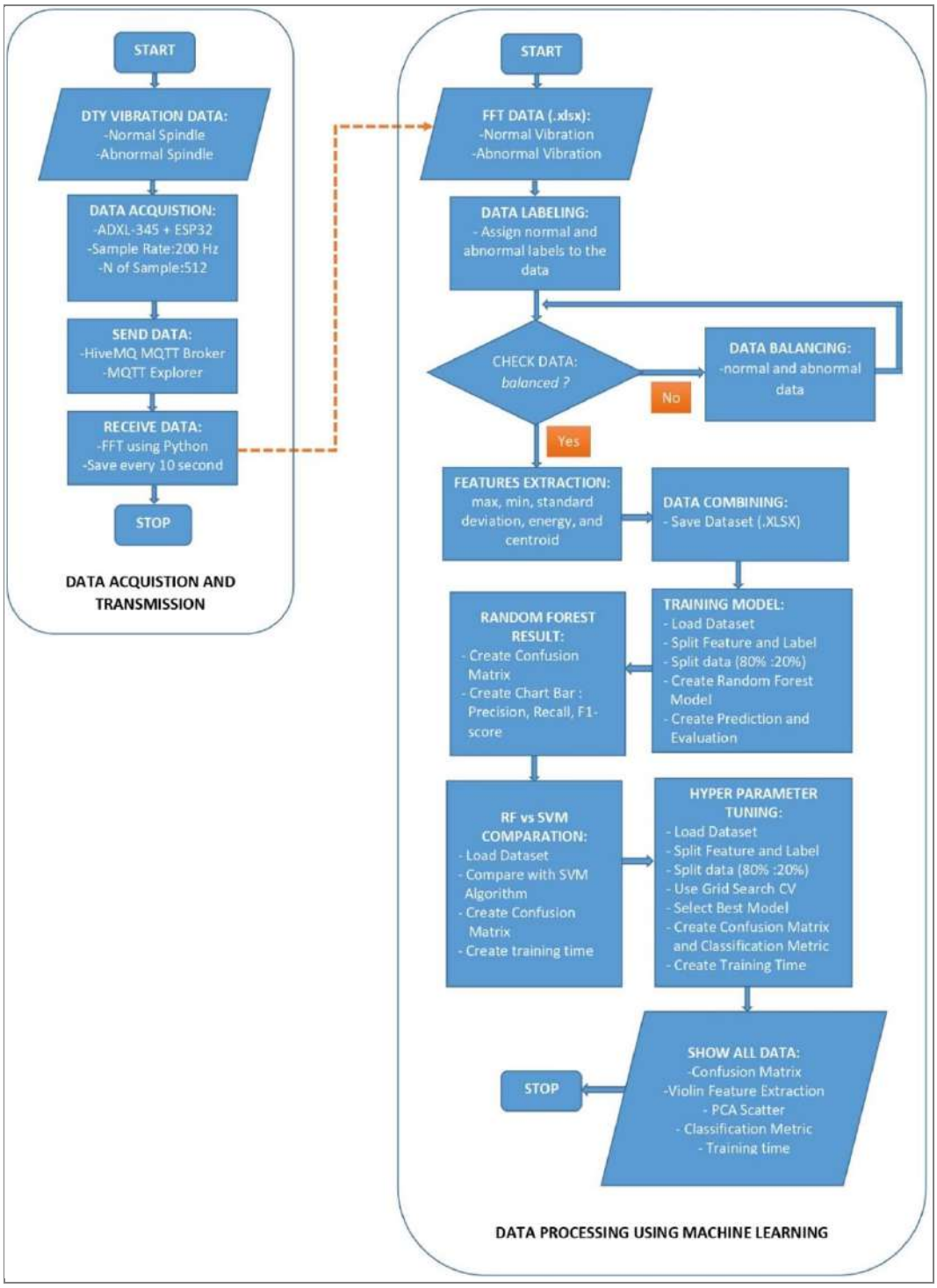

Figure 3. Flow chart of the study method

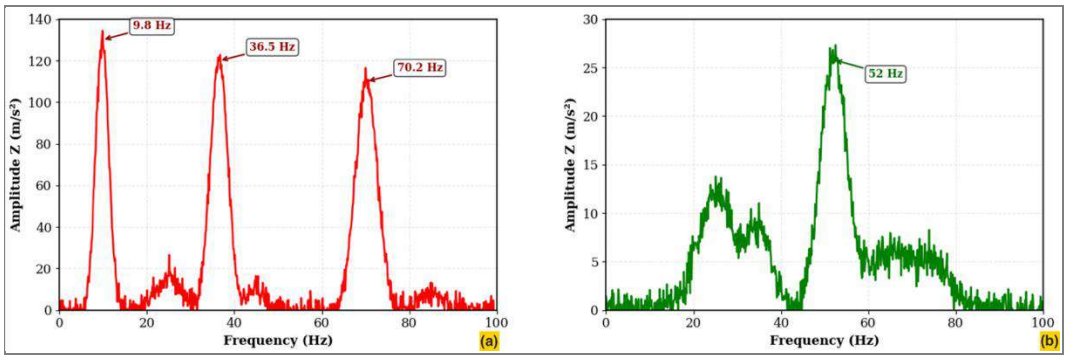

Figure 4. FFT Data sample from: (a) Abnormal vibration; (b) Normal vibration

Figure 4 showed the FFT analysis of vertical (Z-axis) vibration signals from the DTY machine in abnormal and normal operating conditions, respectively. The frequency domain representation signified distinct spectral characteristics between the two conditions. In the abnormal condition (Figure 4a), prominent peaks were observed at approximately 9.8 Hz, 36.5 Hz, and 70.2 Hz, with the highest amplitude reaching nearly 130 m/s². These peaks showed the presence of significant harmonic components, potentially implying mechanical anomalies such as imbalance or looseness. In the normal condition (Figure 4b), vibration amplitudes were significantly lower across the frequency range, with a maximum peak around 25.8 m/s² at approximately 52 Hz. Other minor peaks were present but remained lower than 15 m/s², signifying stable machine behavior with minimal excitation of resonant frequencies.

During the evaluation phase, data transmission via the MQTT protocol was tested using 100 samples, with each measurement repeated in two separate trials. The outcomes of these experiments were shown in Figure 5. The monitoring results obtained through MQTT Explorer were shown in Figure 6. Meanwhile, Table 2 showed the average test measurements during the process.

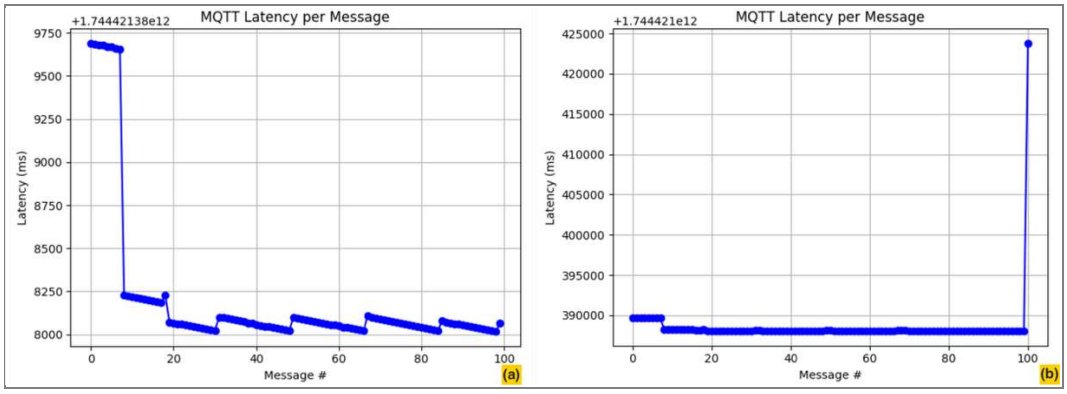

Figure 5. Latency process measurement: (a) First test; (b) Second test

Figure 6. MQTT explorer for data monitoring

Table 2. Final result of data sending latency time via HiveMQ broker

Latency	Times (ms)
Average	20.37
Maximum	23.14
Minimum	18.86

The initial feature extraction process produced 142,592 abnormal and 68,608 normal samples. Following data balancing, both classes were standardized to 68,608 samples each. Despite this adjustment, the dataset remained computationally intensive for RF training, primarily because of the incorporated frequency-domain features. A secondary feature extraction phase was conducted using FFT to decompose the signals into amplitude-frequency representations. Table 3 showed the explanation of the overall results of vibration signal extraction.

Table 3 showed the statistical analysis of vibration features, which included energy and centroid values for the X, Y, as well as Z axes. The table presented the mean, standard deviation, minimum, and maximum values for both normal (label = 0) and abnormal (label = 1) machine conditions, as energy values rose significantly during abnormal operation. For example, X_energy increased from 27,554.93 (normal) to 41,544.33 (abnormal). On the other hand, Z_energy showed the largest jump, from 2,532.32 to 9,098.36. Centroid values changed slightly, where X_centroid increased from 43.19 to 44.58. In addition, Y_centroid had a decrease from 46.98 to 45.33, and Z_centroid stayed near 47.16 in both conditions.

Violin plots (Figure 7) confirmed the trends, showing that abnormal data signified wider distributions and higher medians, specifically for energy features. This signified stronger, more irregular vibration during faults in the process of the analysis.

The PCA scatter plot (Figure 8) showed clear separation between normal (green) and abnormal (red) data clusters. This proved that these features effectively distinguished between machine states for classification.

The performance evaluation of the RF classifier was shown in Figure 9, which signified precision, recall, and F1-score for both normal as well as abnormal classes. The model showed high and balanced performance across both categories, with all metric values exceeding 0.93.

Concerning the normal class, the classifier achieved 0.94 precision, 1.00 recall, and 0.97 F1-score. This showed that all actual normal instances were successfully identified, with a small proportion of abnormal instances incorrectly classified as normal.

Table 3. Statistics of vibration signal extraction features (Units: energy in $(m/s^2)^2$, centroid in Hz)

Features	Class Label	Mean	Std Dev	Min	Max
X_energy	0	27,554.93	18,475.52	1,463.85	95,171.15
X_energy	1	41,544.33	34,292.6	2,645.75	259,728.33
Y_energy	0	1,536.86	1,027.19	110.93	6,406.78
Y_energy	1	2,701.07	2,400.12	112.98	18,714.21
Z_energy	0	2,532.33	1,130.78	155.87	6,952.74
Z_energy	1	9,098.36	13,998.48	185.82	69,319.42
X_centroid	0	43.19	2.91	36.8	48.61
X_centroid	1	44.58	3.17	31.73	51.18
Y_centroid	0	46.98	2.42	41.36	52.22
Y_centroid	1	45.33	2.76	37.38	51.54
Z_centroid	0	47.16	1.97	42.45	51.38
Z_centroid	1	47.16	2.48	36.91	51.82

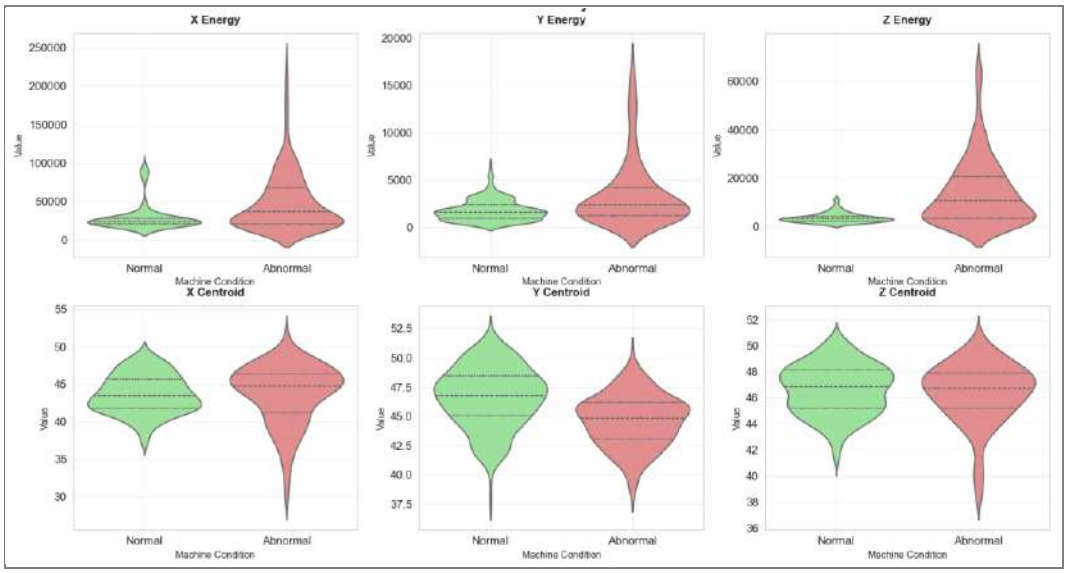

Figure 7. Violin plot of extracted features by class

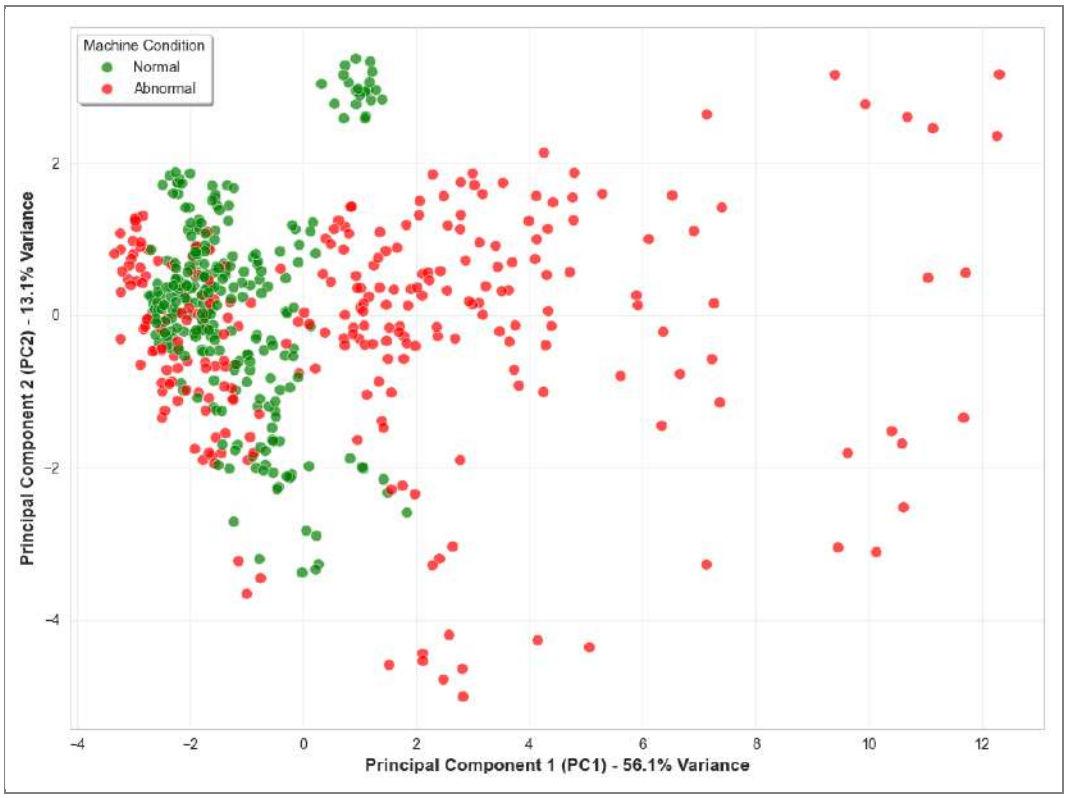

Figure 8. PCA projection of vibration features

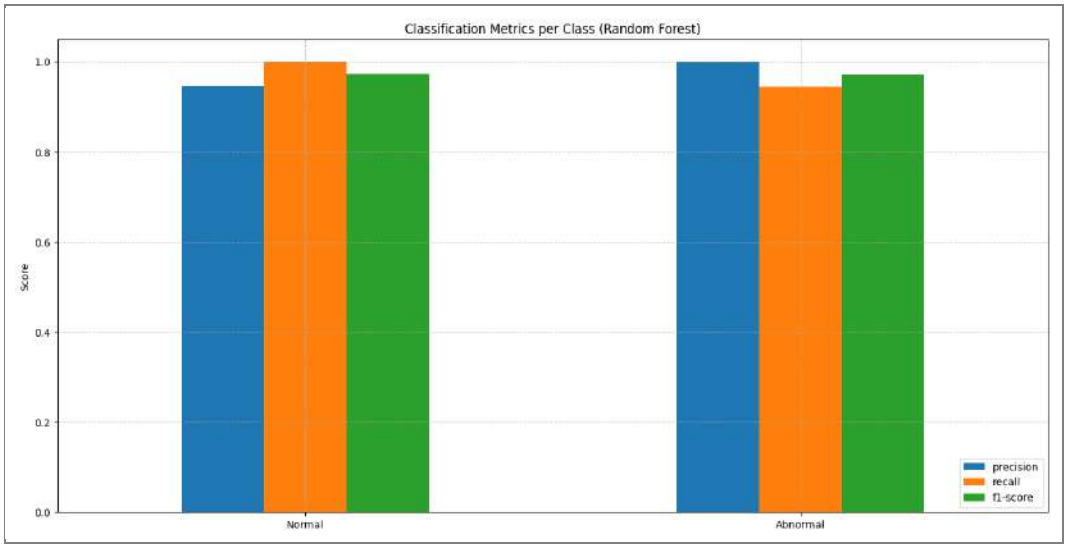

Figure 9. Classification metric

The precision reached 1.00, and the recall was slightly lower at 0.94 for the abnormal class, leading to an F1-score of 0.97. This signified the model was able to perfectly avoid false positives for abnormal conditions, though a few abnormal samples were missed. The results confirmed that the model achieved near-optimal classification in distinguishing between healthy and faulty machine states using the extracted vibration features.

Table 4 showed a comparative summary of classification performance between RF and SVM models in detecting vibration anomalies. RF achieved a total accuracy of 97%, significantly outperforming SVM, which produced only 71% accuracy. Following the process, RF showed high precision, recall, and F1-score for both normal and abnormal classes (≥ 0.94). Meanwhile, SVM showed significant imbalance, with particularly lower recall (0.59) in detecting abnormal conditions.

The confusion matrix (**Figure 10a** and **Figure 10b**) further confirmed the results. The RF classifier correctly predicted 54 normal and 51 abnormal instances, with only 3 misclassified cases. Consequently, SVM misclassified 31 samples, including 9 normal and 22 abnormal instances.

Table 4. Performance comparison between RF and SVM

Metric	Random Forest	SVM
Accuracy	0.97	0.71
Precision (0)	0.95	0.67
Precision (1)	1.00	0.78
Recall (0)	1.00	0.83
Recall (1)	0.94	0.59
F1-score (0)	0.97	0.74
F1-score (1)	0.97	0.67

Table 5. Model training time comparison

Model	Training Time (seconds)
Random Forest	0.1883
Support Vector Machine	0.0229

The training time (**Table 5**) for RF remained acceptable (0.1883 s) despite the higher computational complexity, which was sufficient for deployment in real-time embedded systems. After performing hyperparameter tuning on the RF classifier, the resulting model showed a consistent and high level of classification performance. The confusion matrix (**Figure 11a**) signified that the model correctly identified 54 out of 54 "Normal" instances and 51 out of 54 "Abnormal" instances, leading to a total of 105 correct predictions out of 108 samples.

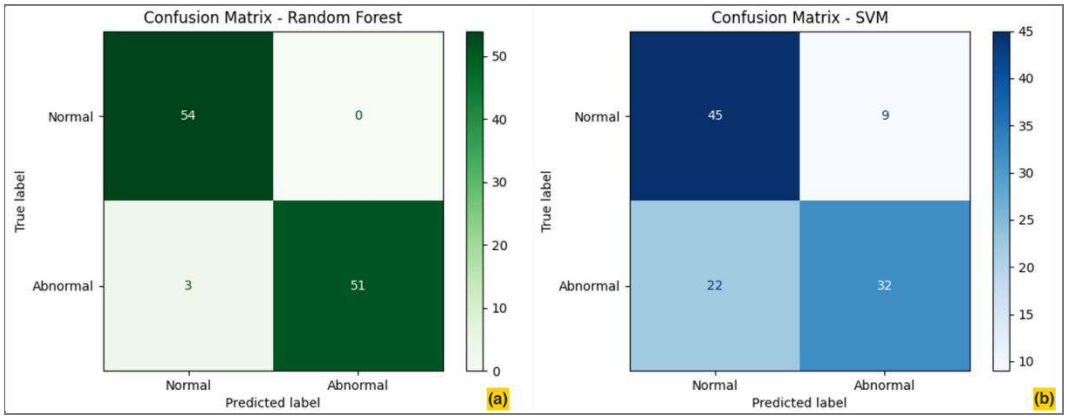

Figure 10. Confusion matrix comparison: (a) Random Forest; (b) SVM

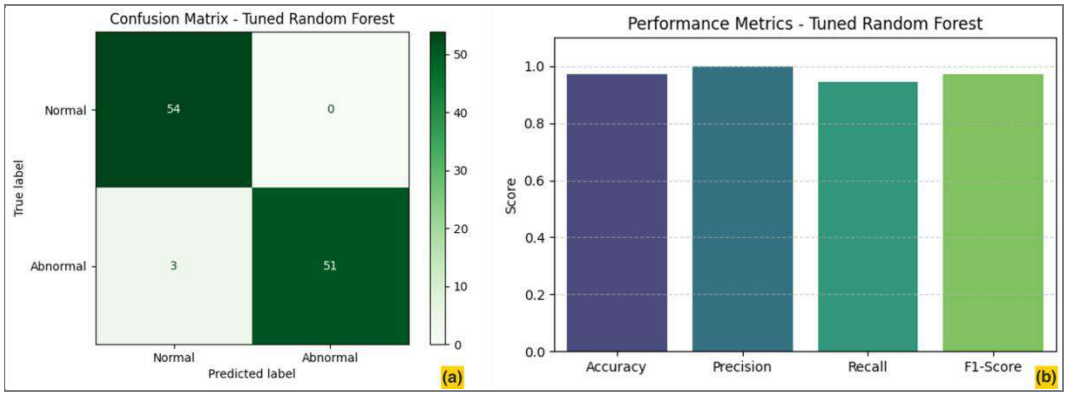

Figure 11.
(a) Confusion matrix;
(b) Performance metrics after Tuning

The performance metrics of the tuned RF model were shown in **Figure 11b**. The model achieved 0.97 accuracy, 1.00 precision, 0.94 recall, and 0.97 F1-score, signifying excellent capability in distinguishing between normal as well as abnormal machine vibration patterns.

The improvement in classification performance came at the cost of increased training time. During the process, the training time of the tuned RF model was 12.6 seconds, which was significantly longer compared to the untuned version (0.1883 seconds) and the SVM model (0.0229 seconds), as shown in **Table 6**.

Table 6.
Training time comparison

Model	Training Time (seconds)
Random Forest (untuned)	0.1883
Support Vector Machine	0.0229
Random Forest (tuned)	12.6

3.2. Discussion

3.2.1. FFT and MQTT Data Transmission Performance

The comparative FFT analysis clearly showed that abnormal machine conditions led to elevated vibration amplitudes and more pronounced spectral peaks. The high-amplitude peaks at 36.5 Hz and 70.2 Hz in the abnormal spectrum corresponded to harmonics of the operating frequency of the machine at 1,500 RPM, which was improved by faults such as misalignment, unbalanced components, or mechanical looseness. The presence of such harmonics was a well-known indicator of deteriorating machine health.

The FFT spectrum of the normal condition showed that the machine operated in acceptable vibration levels, with energy concentrated in a narrow frequency band. The absence of excessive harmonics and the relatively smooth spectrum signified that the machine components were operating in a mechanically sound state.

This difference confirms that frequency-domain analysis is an effective method for early detection of mechanical faults in rotating machinery. These results supported Patil *et al.*'s study, who showed that unbalanced faults signified a dominant frequency characteristic [33]. The distinct spectral signatures observed could be leveraged for automated classification and predictive maintenance strategies using machine learning algorithms.

The performance evaluation of MQTT-based data transmission using ESP32 and ADXL345 sensor showed outstanding latency variations. In the first test (**Figure 5a**), initial messages experienced significantly high latency, with the maximum reaching approximately 9700 ms. However, as the communication stabilized, latency gradually decreased and became consistent at around 8000 ms. This behavior showed that the system required an initial warm-up or setup phase before achieving stable transmission performance.

The second test (**Figure 5b**) showed a stable latency distribution around 389.000 ms, with a sudden extreme spike observed in the 100th message. This anomaly was possibly caused by transient network congestion, processing delays in the microcontroller, or irregularities in timestamp synchronization. Consistent with Mishra *et al.*'s results [34], these results showed that HiveMQ did not outperform Mosquitto and ActiveMQ brokers. Even with this deviation, the total communication remained stable, showing the reliability of HiveMQ for continuous WiFi-based MQTT sensor data transmission. Further optimization was needed to handle such anomalies, specifically for real-time or latency-sensitive applications.

3.2.2. Violin and PCA Scatter Plot Analysis

Both statistical analysis and visualizations showed that energy features were the best indicators of machine faults. When the machine operated abnormally, energy values increased

significantly across all axes, showing stronger and more irregular vibration, as a clear sign of mechanical problems or imbalance.

The higher standard deviation values during faults (such as X_energy increasing from 18,475.52 to 34,292.60) confirmed the result. This showed more variation in vibration patterns when the machine was not working properly. As centroid features changed less dramatically, the features still provided useful information. Moreover, small centroid shifts showed changes in vibration frequencies that could appear before significant energy increases, making the processes valuable for detecting early-stage problems.

Violin plots showed wider, more spread-out distributions for faulty operation, specifically in energy measurements. The PCA plot also signified that both energy and centroid features effectively separated normal as well as abnormal machine states, proving the usefulness of the RF classifier. As a result, combining energy and centroid features enabled reliable fault detection in the vibration monitoring system, including the identification of early warning signs.

3.2.3. Classification Results and Error Implications

In **Figure 9** and **Figure 10a**, the classification results reflected the effectiveness of the feature extraction process and the suitability of the RF algorithm for this task. The perfect recall for the normal class (1.00) showed that the model was highly reliable in detecting non-faulty conditions, critical for avoiding unnecessary maintenance actions.

The perfect precision for the abnormal class (1.00) was equally important, ensuring that the model was certain when flagging a machine as faulty. This is a valuable trait for real-world deployment, where false alarms can be costly or disruptive.

The minor trade-off appeared in the recall of the abnormal class (0.94), signifying that a small portion of faulty cases might be undetected. Even though this performance was still excellent, the model showed an area for potential improvement, such as feature augmentation or ensemble optimization.

3.2.4. Model Comparison between RF and SVM

The analysis showed RF outperformed SVM for vibration data classification, achieving higher accuracy and better handling of both normal as well as fault conditions. The advantage of RF came from its ensemble nature, which combined multiple decision trees to reduce overfitting and improve generalization on noisy, real-world industrial data. RF captured complex non-linear relationships and feature interactions in vibration signals difference from SVM that found a single optimal hyperplane, such as the interplay between energy as well as centroid values across different axes, making it particularly robust for this application.

Theoretical Superiority of RF. Outside the numerical results, the superiority of RF could be attributed to its ensemble architecture, which inherently handled non-linear relationships and feature interactions prevalent in vibration data. RF combined multiple decision trees different from the single hyperplane method of SVM, reducing overfitting and improving robustness to sensor noise as well as outliers. Furthermore, the built-in feature importance assessment of RF automatically prioritized the most discriminative attributes (e.g., Z-axis energy), providing inherent interpretability that SVM lacked.

The results of this study showed superior performance of RF across all key metrics (precision, recall, F1-score). A critical weakness of SVM was its high false-negative rate for faults, a significant risk in industrial settings where missed detections led to machine damage or downtime. Although SVM trained faster, the superior accuracy and reliability of RF were dominant for predictive maintenance systems. As some studies (e.g., Dong *et al*. [35]) reported SVM performing well on specific machine data, these results confirmed that the consistency and balance of RF made the model a more suitable selection for robust, real-world vibration monitoring.

3.2.5. Model Evaluation After Hyperparameter Tuning

After comparing models, RF performed better than SVM, specifically for imbalanced vibration data. The analysis tuned its hyperparameters (such as tree count and depth) using Grid Search CV to improve RF further. The tuned RF showed excellent results, which included the following.

- Correctly classified 54/54 normal cases and 51/54 abnormal cases (**Figure 11a**).
- Only 3 abnormal cases were misclassified.
- Achieved 97% accuracy, perfect precision (1.00), 94% recall, and 97% F1-score (**Figure 11b**).

As tuning improved performance, the process increased training time from 0.22s to 12.6s (**Table 5**). This trade-off was useful as the tuned RF significantly outperformed SVM (97% vs 71% accuracy) and was reliable for real-world use.

As the 12.6s training time presented a challenge for real-time edge model updates, this operation was typically performed offline during model development. For deployed systems, only the inference time was critical, and the prediction latency of RF remained sufficiently low for real-time vibration monitoring. The tuned parameters were deployed to edge devices without requiring on-device retraining, making this method practical for industrial applications where model stability was prioritized over frequent updates.

Benchmarking against Daviran *et al.*'s GA-based hyperparameter tuning showed improved accuracy (up to 100% model identification) [36], though such results remained dataset-dependent and might not generalize across all cases. The experimental outcomes signified that a Grid Search CV-optimized RF classifier was highly effective for machine vibration analysis, making it a suitable candidate for real-world industrial fault detection. To build upon the analysis, subsequent studies could focus on incorporating this model into larger ensembles or using feature selection to reduce computational overhead while maintaining predictive performance.

3.2.6. Limitation and Future Work

This study presented an effective IoT-based method for detecting vibration anomalies in DTY machines using RF classification, as several limitations needed to be addressed. First, the system was tested exclusively on DTY machines in controlled textile manufacturing conditions. Its applicability to other machine types or environments with different load dynamics and rotational speeds remained unverified and required further validation in broader industrial contexts [37]. Second, the analysis heavily relied on Z-axis vibration features, which showed the strongest indication of defects. As this produced high accuracy, fault patterns varied across axes depending on sensor placement and machine configuration. Future work should investigate multi-axis signal fusion to improve robustness [38]. Third, the dataset was limited to 13 spindles over an 8-hour recording period. Though sufficient for initial modeling, a larger and more diverse dataset was needed to improve model generalization and capture rare or long-term fault patterns [39]. Fourth, hyperparameter tuning improved accuracy but significantly increased training time, from 0.18 s to 12.6 s. This trade-off might hinder real-time applications in edge computing environments with limited resources. Similar concerns applied to the observed latency fluctuations during MQTT-based data transmission, specifically under unstable networks or higher sampling rates [40]. Fifth, the use of FFT-based features provided strong discriminatory power but demanded high computational effort. Lightweight alternatives such as wavelet transforms or statistical moment features could reduce processing time without compromising accuracy [41].

This study did not consider external environmental variables such as temperature, humidity, or electromagnetic interference, which may affect sensor readings. Incorporating environmental data might improve system reliability under real-world operating conditions [42], and finally, model comparison was limited to SVM. Future evaluations should include other state-of-the-art models such as gradient boosting, lightweight neural networks, or hybrid ensemble methods to better assess the relative performance of the system [43]. In addition, future studies should also include collecting larger datasets across diverse industrial settings, optimizing the model for edge devices, improving resilience to network variability, incorporating environmental sensors, and conducting field trials to assess system performance in live production environments.

4. Conclusion

In conclusion, the study successfully developed an IoT-based vibration monitoring system for DTY machines, leveraging the ADXL345 sensor, ESP32 microcontroller, MQTT protocol, and a tuned RF classifier. By combining FFT-based feature extraction and machine learning, the system achieved high accuracy (97%) in distinguishing abnormal vibration, significantly outperforming SVM. The Z-axis vibration data and energy from the ADXL345 sensor were identified as critical indicators of machine faults, associated with industrial observations. Despite increased computational time post-hyperparameter tuning (12.6 seconds), the reliability and precision of the model justified its use in real-world applications. The MQTT protocol ensured efficient data transmission with minimal latency, validating the feasibility of the system for real-time monitoring. This work advanced predictive maintenance in textile manufacturing by offering a robust, scalable solution that reduced dependency on manual inspections and mitigated operational disruptions.

Future study could explore ensemble methods or edge computing to further optimize performance and deployment efficiency.

Authors' Declaration

Authors' contributions and responsibilities - ***Deni Kurnia*** was responsible for data collection from the DTY machines, performing data analysis, and preparing the initial draft of the manuscript. ***Agus Sutanto*** supervised the overall research process, including the data collection framework and the structure and clarity of the manuscript. ***Hanif Fakhrurroja*** contributed to the technical validation and performance evaluation of the machine learning algorithms applied in the study. ***Lovely Son*** ensured accurate calibration and operational validation of the vibration sensors installed on the machines.

Funding – No funding information from the authors.

Availability of data and materials - All data is available from the authors.

Competing interests - The authors declare no competing interests.

Additional information – No additional information from the authors.

References

[1] N. Jamil, M. F. Hassan, S. K. Lim, and A. R. Yusoff, "Predictive maintenance for rotating machinery by using vibration analysis," *Journal of Mechanical Engineering and Sciences*, vol. 15, no. 3, pp. 8289–8299, Sep. 2021, doi: 10.15282/jmes.15.3.2021.07.0651.

[2] M. Romanssini, P. C. C. de Aguirre, L. Compassi-Severo, and A. G. Girardi, "A Review on Vibration Monitoring Techniques for Predictive Maintenance of Rotating Machinery," *Eng*, vol. 4, no. 3, pp. 1797–1817, Jun. 2023, doi: 10.3390/eng4030102.

[3] D. Jung, Z. Zhang, and M. Winslett, "Vibration Analysis for IoT Enabled Predictive Maintenance," in *2017 IEEE 33rd International Conference on Data Engineering (ICDE)*, IEEE, Apr. 2017, pp. 1271–1282. doi: 10.1109/ICDE.2017.170.

[4] M. Iliyas Ahmad, Y. Yusof, M. E. Daud, K. Latiff, A. Z. Abdul Kadir, and Y. Saif, "Machine monitoring system: a decade in review," *The International Journal of Advanced Manufacturing Technology*, vol. 108, no. 11–12, pp. 3645–3659, Jun. 2020, doi: 10.1007/s00170-020-05620-3.

[5] V. J. F. Alexandre, W. P. Boshoff, and R. Combrinck, "Damage evaluation and mechanisms of textile reinforced concrete during telescopic failure," *Construction and Building Materials*, vol. 403, p. 133055, Nov. 2023, doi: 10.1016/j.conbuildmat.2023.133055.

[6] Afzeri, D. Kurnia, M. N. Hakim, and I. S. Nurmala, "Implementation of FFT in Industrial Induction Motor Monitoring via Mobile Phone," *Journal of Applied Science and Advanced Engineering*, vol. 1, no. 1, pp. 5–10, Jan. 2023, doi: 10.59097/jasae.v1i1.8.

[7] D. Goyal, A. Choudhary, B. S. Pabla, and S. S. Dhami, "Support vector machines based non-contact fault diagnosis system for bearings," *Journal of Intelligent Manufacturing*, vol. 31, no. 5, pp. 1275–1289, Jun. 2020, doi: 10.1007/s10845-019-01511-x.

[8] L. Yuan, D. Lian, X. Kang, Y. Chen, and K. Zhai, "Rolling Bearing Fault Diagnosis Based on Convolutional Neural Network and Support Vector Machine," *IEEE Access*, vol. 8, pp. 137395–137406, 2020, doi: 10.1109/ACCESS.2020.3012053.

[9] Q. Hu, X.-S. Si, Q.-H. Zhang, and A.-S. Qin, "A rotating machinery fault diagnosis method based on multi-scale dimensionless indicators and random forests," *Mechanical Systems and Signal Processing*, vol. 139, p. 106609, May 2020, doi: 10.1016/j.ymssp.2019.106609.

[10] G. Guo, X. Cui, and B. Du, "Random-Forest Machine Learning Approach for High-Speed Railway Track Slab Deformation Identification Using Track-Side Vibration Monitoring," *Applied Sciences*, vol. 11, no. 11, p. 4756, May 2021, doi: 10.3390/app11114756.

[11] F. A. D. N. Setúbal, S. de S. Custódio Filho, N. S. Soeiro, A. L. A. Mesquita, and M. V. A. Nunes, "Force Identification from Vibration Data by Response Surface and Random Forest Regression Algorithms," *Energies*, vol. 15, no. 10, p. 3786, May 2022, doi: 10.3390/en15103786.

[12] X. Zhao and M. Jia, "A novel unsupervised deep learning network for intelligent fault diagnosis

of rotating machinery," *Structural Health Monitoring*, vol. 19, no. 6, pp. 1745–1763, Nov. 2020, doi: 10.1177/1475921719897317.

[13] G. Toh and J. Park, "Review of Vibration-Based Structural Health Monitoring Using Deep Learning," *Applied Sciences*, vol. 10, no. 5, p. 1680, Mar. 2020, doi: 10.3390/app10051680.

[14] Y. Zou, Y. Zhang, and H. Mao, "Fault diagnosis on the bearing of traction motor in high-speed trains based on deep learning," *Alexandria Engineering Journal*, vol. 60, no. 1, pp. 1209–1219, Feb. 2021, doi: 10.1016/j.aej.2020.10.044.

[15] A. Kumar, G. Vashishtha, C. P. Gandhi, Y. Zhou, A. Glowacz, and J. Xiang, "Novel Convolutional Neural Network (NCNN) for the Diagnosis of Bearing Defects in Rotary Machinery," *IEEE Transactions on Instrumentation and Measurement*, vol. 70, pp. 1–10, 2021, doi: 10.1109/TIM.2021.3055802.

[16] N. V. S. Shankar, V. S. N. Venkata Ramana, A. Sravani, P. Sreenivasulu, and K. Sriram Vikas, "IoT for vibration measurement in engineering research," *Materials Today: Proceedings*, vol. 59, pp. 1792–1796, 2022, doi: 10.1016/j.matpr.2022.04.380.

[17] M. Babiuch, P. Foltynek, and P. Smutny, "Using the ESP32 Microcontroller for Data Processing," in *2019 20th International Carpathian Control Conference (ICCC)*, IEEE, May 2019, pp. 1–6. doi: 10.1109/CarpathianCC.2019.8765944.

[18] S. Quincozes, T. Emilio, and J. Kazienko, "MQTT Protocol: Fundamentals, Tools and Future Directions," *IEEE Latin America Transactions*, vol. 17, no. 09, pp. 1439–1448, Sep. 2019, doi: 10.1109/TLA.2019.8931137.

[19] Y. Liu, Y. Wang, and J. Zhang, "New Machine Learning Algorithm: Random Forest," in *Lecture Notes in Computer Science (including subseries Lecture Notes in Artificial Intelligence and Lecture Notes in Bioinformatics)*, vol. 7473 LNCS, 2012, pp. 246–252. doi: 10.1007/978-3-642-34062-8_32.

[20] M. Hasibuzzaman, A. Shufian, R. K. Shefa, R. Raihan, J. Ghosh, and A. Sarker, "Vibration Measurement & Analysis Using Arduino Based Accelerometer," in *2020 IEEE Region 10 Symposium (TENSYMP)*, IEEE, 2020, pp. 508–512. doi: 10.1109/TENSYMP50017.2020.9230668.

[21] A. Sutanto, D. Kurnia, H. Fakhrurroja, and N. Roni Wibowo, "Real-Time Identification of Yarn Irregularities on DTY Machine Through Vibration Monitoring," *Jurnal Polimesin*, vol. 22, no. 6, p. 693, Dec. 2024, doi: 10.30811/jpl.v22i6.5847.

[22] O. Khouili, M. Hanine, M. Louzazni, and W. J. Obidallah, "Smart solar power prediction using an FFT-Infused ShuffleNet regressor: A high-accuracy lightweight framework," *International Journal of Electrical Power & Energy Systems*, vol. 172, p. 111240, Nov. 2025, doi: 10.1016/j.ijepes.2025.111240.

[23] R. Tanious and R. Manolov, "Violin plots as visual tools in the meta-analysis of Single-Case Experimental Designs," *Methodology*, vol. 18, no. 3, pp. 221–238, Sep. 2022, doi: 10.5964/meth.9209.

[24] J. Camacho, J. Picó, and A. Ferrer, "Data understanding with PCA: Structural and Variance Information plots," *Chemometrics and Intelligent Laboratory Systems*, vol. 100, no. 1, pp. 48–56, Jan. 2010, doi: 10.1016/j.chemolab.2009.10.005.

[25] H. A. Salman, A. Kalakech, and A. Steiti, "Random Forest Algorithm Overview," *Babylonian Journal of Machine Learning*, vol. 2024, pp. 69–79, Jun. 2024, doi: 10.58496/BJML/2024/007.

[26] G. Biau and E. Scornet, "A random forest guided tour," *TEST*, vol. 25, no. 2, pp. 197–227, Jun. 2016, doi: 10.1007/s11749-016-0481-7.

[27] J.-M. Nguyen *et al.*, "Random forest of perfect trees: concept, performance, applications and perspectives," *Bioinformatics*, vol. 37, no. 15, pp. 2165–2174, Aug. 2021, doi: 10.1093/bioinformatics/btab074.

[28] V. Jakkula, "Tutorial on Support Vector Machine (SVM)," School of EECS, Washington State University, 2011.

[29] Y. Zhang, "Support Vector Machine Classification Algorithm and Its Application," in *Communications in Computer and Information Science*, vol. 308 CCIS, no. PART 2, 2012, pp. 179–186. doi: 10.1007/978-3-642-34041-3_27.

[30] S. Salcedo-Sanz, J. L. Rojo-Álvarez, M. Martínez-Ramón, and G. Camps-Valls, "Support vector machines in engineering: an overview," *WIREs Data Mining and Knowledge Discovery*, vol. 4,

no. 3, pp. 234–267, May 2014, doi: 10.1002/widm.1125.

[31] Y. Zhao, W. Zhang, and X. Liu, "Grid search with a weighted error function: Hyper-parameter optimization for financial time series forecasting," *Applied Soft Computing*, vol. 154, p. 111362, Mar. 2024, doi: 10.1016/j.asoc.2024.111362.

[32] F. Budiman, "SVM-RBF Parameters Testing Optimization Using Cross Validation and Grid Search to Improve Multiclass Classification," *Scientific Visualization*, vol. 11, no. 1, pp. 80–90, 2019, doi: 10.26583/sv.11.1.07.

[33] S. S. Patil and J. A. Gaikwad, "Vibration analysis of electrical rotating machines using FFT: A method of predictive maintenance," in *2013 Fourth International Conference on Computing, Communications and Networking Technologies (ICCCNT)*, IEEE, Jul. 2013, pp. 1–6. doi: 10.1109/ICCCNT.2013.6726711.

[34] B. Mishra, B. Mishra, and A. Kertesz, "Stress-testing mqtt brokers: A comparative analysis of performance measurements," *Energies*, vol. 14, no. 18, pp. 1–20, 2021, doi: 10.3390/en14185817.

[35] L. Dong, X. Li, M. Xu, and Q. Li, "Comparisons of random forest and Support Vector Machine for predicting blasting vibration characteristic parameters," *Procedia Engineering*, vol. 26, pp. 1772–1781, 2011, doi: 10.1016/j.proeng.2011.11.2366.

[36] M. Daviran, A. Maghsoudi, R. Ghezelbash, and B. Pradhan, "A new strategy for spatial predictive mapping of mineral prospectivity: Automated hyperparameter tuning of random forest approach," *Computers and Geosciences*, vol. 148, no. May 2020, p. 104688, 2021, doi: 10.1016/j.cageo.2021.104688.

[37] Y. Deng, Y. Zhao, H. Ju, T.-H. Yi, and A. Li, "Abnormal data detection for structural health monitoring: State-of-the-art review," *Developments in the Built Environment*, vol. 17, p. 100337, Mar. 2024, doi: 10.1016/j.dibe.2024.100337.

[38] S. Liu *et al.*, "Multi-feature fusion for fault diagnosis of rotating machinery based on convolutional neural network," *Computer Communications*, vol. 173, pp. 160–169, May 2021, doi: 10.1016/j.comcom.2021.04.016.

[39] A. Kafeel *et al.*, "An Expert System for Rotating Machine Fault Detection Using Vibration Signal Analysis," *Sensors*, vol. 21, no. 22, p. 7587, Nov. 2021, doi: 10.3390/s21227587.

[40] A. R. Alkhafajee, A. M. A. Al-Muqarm, A. H. Alwan, and Z. R. Mohammed, "Security and Performance Analysis of MQTT Protocol with TLS in IoT Networks," in *2021 4th International Iraqi Conference on Engineering Technology and Their Applications (IICETA)*, IEEE, Sep. 2021, pp. 206–211. doi: 10.1109/IICETA51758.2021.9717495.

[41] J. Shi, G. Si, S. Li, B. Oresanya, and Y. Zhang, "Feature extraction based on the fractional Fourier transform for vibration signals with application to measuring the load of a tumbling mill," *Control Engineering Practice*, vol. 84, pp. 238–246, Mar. 2019, doi: 10.1016/j.conengprac.2018.11.012.

[42] S. L. Ullo and G. R. Sinha, "Advances in Smart Environment Monitoring Systems Using IoT and Sensors," *Sensors*, vol. 20, no. 11, p. 3113, May 2020, doi: 10.3390/s20113113.

[43] R. Kumar, K. S. Sangwan, C. Herrmann, R. Ghosh, and M. Sangwan, "Development and comparison of machine-learning algorithms for anomaly detection in 3D printing using vibration data," *Progress in Additive Manufacturing*, vol. 9, no. 2, pp. 529–541, Apr. 2024, doi: 10.1007/s40964-023-00472-1.